# UNUSUAL TEMPERATURE DEPENDENCE OF COERCIVITY IN ε-$Fe_2O_3$ PHASE

NIKOLIĆ N. Violeta[1], TADIĆ Marin[1], MRAKOVIĆ Ana[1], SPASOJEVIĆ Vojislav[1]

[1] *University of Belgrade - Vinča Institute of Nuclear Sciences, Condensed Matter Physics Laboratory, Belgrade, Republic of Serbia, violeticanik@gmail.com*

**Abstract**

Nano iron oxides have been intensively investigated due to their various potential biomedical applications. ε-$Fe_2O_3$ phase exerted internal coercivity value up to ~20 kOe, high Curie temperature ( $T_c$= 510 K), and magnetoelectric character. Accordingly, epsilon phase is recognized as a suitable material for medical spintronic biosensors production, that present important part for the lab-on-a-chip systems. Noteworthy, ε-$Fe_2O_3$ phase exerts peculiar magnetic behavior. To get better insight into the magnetism of this material, ε-$Fe_2O_3$/$SiO_2$ sample was prepared by the combination of the sol-gel synthesis and microemulsion method ($T_{ann}$=1050 °C, $t_{ann}$= 4h). Afterwards, the sample was exposed to post-annealing treatment at 100 °C and 200 °C. Synthesized material was preliminary examined by XRD and SQUID techniques. Coercivity changes, induced by the post-annealing temperature oscillations, were monitored by hysteretic measurements. Sample annealed at 1050 °C for 4h, showed coercivity ~20 kOe. The same sample performed to the post-annealing treatment at 100 °C, exerted significantly decreased coercivity (~1600 Oe). Further rise of the post-annealing temperature (200 °C) resulted in the increased coercivity ~15 kOe. Obtained study showed that there is insufficient knowledge concerning the ε-$Fe_2O_3$ coercivity changes of the polymorph. The more detailed investigation will be conducted, in order to advance the control of the epsilon phase magnetic properties.

**Keywords:** ε-$Fe_2O_3$ phase, coercivity, phase transformations

## 1. INTRODUCTION

ε-$Fe_2O_3$ is recognized as a potential futuristic material, for application in electronic and storage technologies [1-6], since this $Fe_2O_3$ polymorph can achieve very high room-temperature coercivity, up to 20 kOe [7-13]. ε-$Fe_2O_3$ phase presents the "youngest" of iron (III) oxides, whether its strucutre was completely described in 1998, by Tronc et al [14]. The usage of ε-$Fe_2O_3$ material is still futuristic, since the investigation of this iron oxide polymorph is faced with a lot of challenges. Up today, it is not known how to prepare pure ε-$Fe_2O_3$ phase. Because of the wide particle size distribution and pronounced thermal instability, ε-$Fe_2O_3$ phase is usually obtained in the combination with the other iron (III) oxide traces, such as γ-$Fe_2O_3$ or α-$Fe_2O_3$ phase [7,12]. Magnetism of the ε-$Fe_2O_3$ phase is still open question. According to the literature data, synthesized ε-$Fe_2O_3$ phase can behave as a room-temperature: canted antiferromagnet [15], collinear ferrimagnet [16], non-collinear ferrimagnet [17], or to behave superparamagnetic behavior [18]. Also, in the literature is presented confusion regarded room temperature coercivity value of the ε-$Fe_2O_3$ phase, that presents the most important property for commercial usage of the ε-$Fe_2O_3$. To get deeper insight in the ε-$Fe_2O_3$ phase transformations and its temperature dependent coercivity behavior, we conducted a presented study. Performed research presents the continuation of the published study devoted to the investigation of the ε-$Fe_2O_3$ phase coercivity temperature dependence [19]. Nikolic et al. synthesized ε-$Fe_2O_3$ nanoparticles in a silica matrix [19]. The nanoparticles were examined by XRD, TEM and SQUID measurements. The ε-$Fe_2O_3$ phase was subjected to the thermal treatment covering a wide range of different post-annealing temperatures: 200 °C, 500 °C, 750 °C, 1000 °C, and 1100 °C. Hysteretic loops were measured, and coercivity field ($H_c$) value was used as a tool for monitoring ε-$Fe_2O_3$ phase transformations.

In this study, ε-$Fe_2O_3$ $H_c$ behavior in the narrow post-annealing temperature range was investigated. Hysteretic measurements were conducted in order to follow the temperature dependent coercivity behavior of the ε-$Fe_2O_3$ phase post-annealed at 100 °C and 200 °C.

## 2. EXPERIMENTAL

### 2.1. Structural and magnetic characterization

The phase composition of the samples was analyzed by powder X-ray diffraction using a Rigaku RINT-TTRIII diffractometer, with Cu-Kα radiation of λ=1.5406 A. M(H) curves measured at 200 K, were investigated by a superconducting quantum interference device (SQUID) magnetometer from Quantum Design MPMS 7.

### 2.2. Synthesis

Synthesis of the ε-$Fe_2O_3$/$SiO_2$ nanoparticles involved combination of microemulsion method and sol-gel, since this method is recognized as an optimal to obtain ε-$Fe_2O_3$ phase as a single phase, with a high yield [20]. Two identical micelles, containing CTAB/n-isooctane/1-butanol/water in molar ratio: 0.03/0.33/0.12/1.00, were prepared. The precursors containing $Fe^{3+}$ ions and $Sr^{2+}$ ions were added into the first micelle, while ammonia was injected into the second micelle [19]. Afterwards, 0.02 mol TEOS was dropped into the solution, prepared by mixing two micelles. Solution was stirred at room temperature for 24h. Precipitate was collected by centrifugation, and washed with chloroform and methanol few times. Thereafter, precipitate was dried at 80 °C for 14h. The ε-$Fe_2O_3$ phase was obtained by annealing dried precipitate at 1050 °C for 4h. Synthesized ε-$Fe_2O_3$/$SiO_2$ nanoparticles were performed to the post-annealing treatment at chosen temperatures: 100 °C and 200 °C, for 3h. Samples were denoted as $S_{1050}$ (as-prepared ε-$Fe_2O_3$ phase), $S_{1050}$100 (ε-$Fe_2O_3$ phase post-annealed at 100 °C), and $S_{1050}$200 (ε-$Fe_2O_3$ phase post-annealed at 200 °C).

## 3. RESULTS AND DISCUSSION

XRD patterns of the as-prepared ε-$Fe_2O_3$/$SiO_2$ phase, $S_{1050}$100, and $S_{1050}$200 are depicted at **Figure 1**.

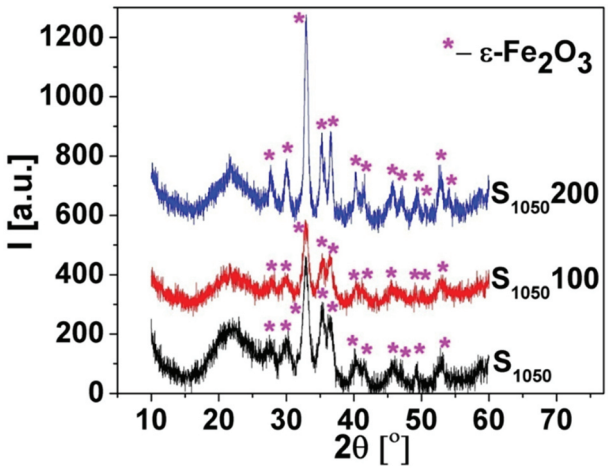


**Figure 1** Diffraction patterns of the post-annealing samples: $S_{1050}$, $S_{1050}$100, $S_{1050}$200. Symbols correspond to: *- ε-$Fe_2O_3$

Diffraction patterns revealed the same composition of the investigated samples. XRD measurements showed that the only observed iron (III) oxide phase is ε-$Fe_2O_3$ phase (JCPDS: PDF no: 16-653, orthorhombic structure, space group $Pna2_1$); traces of the other $Fe_2O_3$ polymorphs were not observed. The Scherrer equation was used to determine crystallite size of the ε-$Fe_2O_3$ phase. Half width was estimated according to

the position of the most pronounced maxima, centered at 2θ angle position: 36.67°. Average crystallite size of the as-prepared ε-$Fe_2O_3$ phase was 6.6 nm. After applying thermal treatment at 100 °C, size of the ε-$Fe_2O_3$ particles was 8 nm, while post-annealing treatment at 200 °C brings to the further growth of the particles; determined ε-$Fe_2O_3$ crystallite size was 14 nm. XRD analysis confirmed strong impact of the thermal treatment onto the growth of the ε-$Fe_2O_3$ nanoparticles.

**Figure 2** presents hysteretic loops of the samples $S_{1050}$ and $S_{1050}$200 (left and right, respectively). Both samples showed very high coercivity value, characteristic for the ε-$Fe_2O_3$ phase prepared by the combination of the micelle and sol-gel method [9, 10, 11, 20, 21]. Sample $S_{1050}$ achieved coercivity ~20 kOe. Sample $S_{1050}$200 also exerted high coercivity (~15 kOe), although somewhat lowered, in comparison to the as-prepared ε-$Fe_2O_3$ phase coercivity. On the basis of literature data, observed coerivity decrease was ascribed to the partial ε-$Fe_2O_3$ to α-$Fe_2O_3$ phase transformation [12, 19, 23].

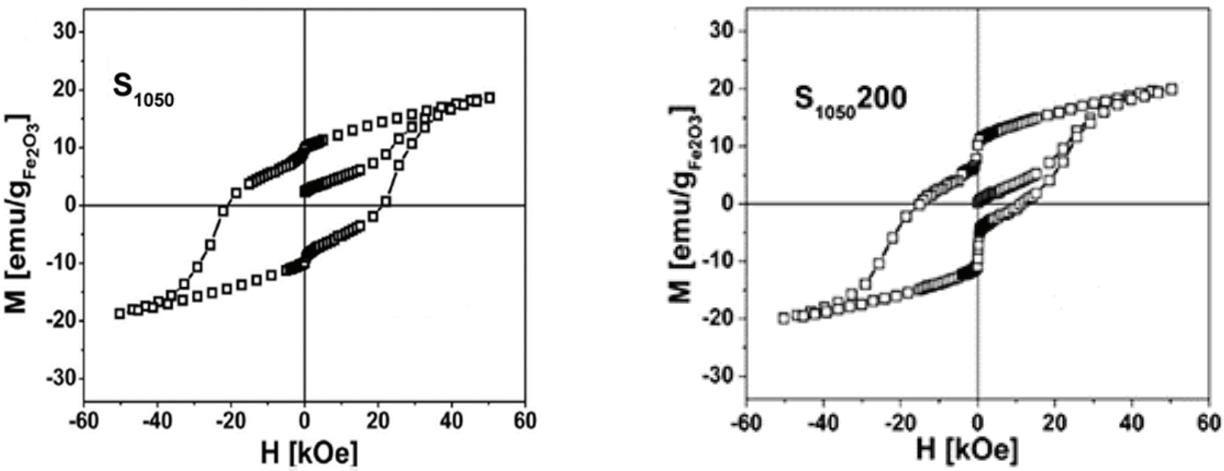


**Figure 2** M(H) curves of the sample $S_{1050}$ (left); M(H) curves of the sample $S_{1050}$200 (right)

Hysteresis of the ε-$Fe_2O_3$ phase performed to post-annealing treatment at 100 °C is shown at **Figure 3**. Contrary, post-annealing process at this temperature brings to the prominent narrowing of the hysteretic loop and revealed the surprising drop of the coercivity field value (~Hc 1600 Oe).

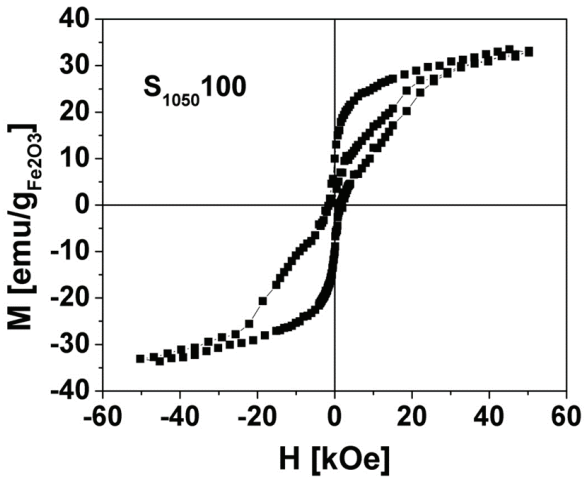


**Figure 3** M(H) curves of the sample $S_{1050}$100

The values of the hysteretic loop parameters are presented in the **Table 1**.

**Table 1** The values of coercivity, saturation and remanent magnetization of the investigated samples

| Sample | $H_c$ [Oe] | $M_s$ [emu/g] | $M_r$ [emu/g] |
|---|---|---|---|
| $S_{1050}$ | 21 290 | 18.4 | 9.7 |
| $S_{1050}100$ | 1 611 | 32.9 | 10.0 |
| $S_{1050}200$ | 15 056 | 20.0 | 10.2 |

Here is important to compare observed coercivity behavior with the results of the former study, related to the investigation of the variations in the room-temperature coercivity field value for the wide range of the post-annealing temperatures: 200 °C, 500 °C, 750 °C, 1000 °C, and 1100 °C [19]. Experimental data revealed decreasing coercivity in the post-annealed samples up to the 750 °C, followed by an observation of a surprising jump in coercivity at 1000 °C. Observed coercivity alteration were explained in the term of the ε-$Fe_2O_3$ phase transformations. Expected progressive decrease of the $H_c$ is ascribed to the ε-$Fe_2O_3$ → α-$Fe_2O_3$ phase transformations. From the other side, peculiar $H_c$ jump appeared due to the ε-$Fe_2O_3$ nanoparticles re-formation. Re-formation mechanism is presented as a consequence of the wide particle size distribution. Annealing treatment at 1000 °C initiated growth of the small γ-$Fe_2O_3$ nanoparticles (< 10 nm), and forced their conversion into the ε-$Fe_2O_3$ phase. Presence of the small γ-$Fe_2O_3$ nanoparticles was not observed by XRD measurements, since maghemite nanoparticles are presented within the samples in traces. Noteworthy, it was highlighted that the appearance of the ε-$Fe_2O_3$ phase depends on physical properties of the $SiO_2$ matrix. Transformation of the $SiO_2$ matrix strongly affected magnetic behavior of the investigated samples, that is confirmed by measuring coercivity of the sample treated at 1100 °C. At this temperature is observed completion of the ε-$Fe_2O_3$ → α-$Fe_2O_3$ phase transformation, as well as crystallization of the amorphous silica matrix into quartz and cristobalite [19].

Compared to the results obtained in the previous study, **Figures 2** and **3** presents very interesting experimental data concerning the post-annealing temperature dependent ε-$Fe_2O_3$ phase coercivity. If we recall XRD patterns of the investigated samples (**Figure 1**), the obtained results undoubtedly pointing out that the observed coercivity alterations can not be ascribed to the ε-$Fe_2O_3$ phase transformations. Considering the coercivity behavior shown in **Figures 2** and **3**, dependency of coercivity on the post-annealed temperatures is redefined (**Figure 4**).

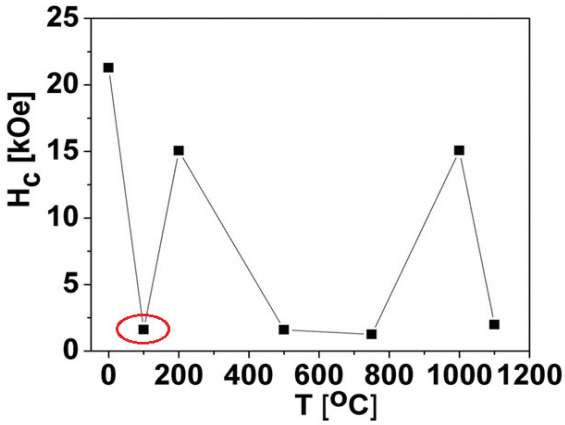


**Figure 4** Dependence of coercivity on the post-annealed temperatures

Based on the conducted XRD and SQUID measurements, it is very difficult to explain precize origin of the coercivity variations. From the literature is known that the coercivity field value can be affected by the huge agglomerates formation, that influences the hysteretic loop parameters and give rise to the increase of the superparamagnetic fraction of the ε-$Fe_2O_3$ phase [22, 23]. This could be one of the possible explanations of the ε-$Fe_2O_3$ phase coercivity variations, although it has to be approved or denied by the further characterization of the samples.

## 4. CONCLUSION

Performed study showed unusual non-monotonic behavior of the temperature dependent ε-$Fe_2O_3$ phase coercivity. Investigated samples were prepared by combination of the microemulsion and sol-gel method. As-prepared ε-$Fe_2O_3$ nanoparticles were exposed to the post-annealing treatment at 100 °C and 200 °C. XRD study showed that samples consist of the ε-$Fe_2O_3$ phase, as the only observed $Fe_2O_3$ polymorph. Calculation of the average crystallite size of the ε-$Fe_2O_3$ phase confirmed growth of the ε-$Fe_2O_3$ particles, initiated by the post-annealing treatment. Recording of the hysteretic curves pointed to the sharp $H_c$ alterations. As-prepared ε-$Fe_2O_3$ phase exerts high coercivity (21.3 kOe). Post-annealing treatment at 100 °C brings to the abruptly drop of coercivity (1611 Oe), while further increase of the post-annealing temperature (200 °C), resulted in the significant coercivity jump (15.1 kOe). To get final remark about the ε-$Fe_2O_3$ phase magnetism and it's temperature dependent coercivity behavior, this research has to be continued by the use of the other measurement techniques.

## ACKNOWLEDGEMENTS

***The authors acknowledge financial support of the Serbian Ministry of Education, Technology and Science (Grant No. III 45015).***

## REFERENCES

[1] OHKOSHI, S., NAMAI, A., IMOTO, K., YOSHIKIYO, M., TARORA, W., NAKAGAWA, K., KOMINE, M., MIYAMOTO, Y., NASU, T., OKA, S., TOKORO, H. Nanometer-size hard magnetic ferrite exhibiting high optical-transparency and nonlinear optical magnetoelectric e□ect, *Scientific Reports*, 2015, vol. 5, no.14414, pp.1-9.

[2] CARRARO, G., GASPAROTTO, A., MACCATO, C., GOMBAC, V., ROSS, F., MONTINI, T., PETER, D., BONTEMPI, E., SADA, C., BARRECA, D., FORNASIERO, P. Solar $H_2$ generation via ethanol photo reforming on ε-$Fe_2O_3$ nanorod arrays activated by Ag and Au nanoparticles, *RSC Advances*, 2014, vol.4, no.3, pp. 32174-32179.

[3] PEETERS, D. BARRECA, D., CARRARO, G., COMINI, E., GASPAROTTO, A., MACCATO, C. SADA, C., SBERVEGLIERI, G. Au/ε-$Fe_2O_3$ nanocomposites as selective NO2 gas sensors, *Journal of Physical Chemistry C*, 2014, vol. 118, no. 22, pp. 11813-11819.

[4] M. YOSHIKIYO, M., NAMAI, A., NAKAJIMA, M., YAMAGUCJI, K., SUEMOTO, T., OHKOSHI, S. High-frequency milimeter wave absorption of indium-substituted ε-$Fe_2O_3$ spherical nanoparticles, *Journal of Applied Physics*, 2014, vol. 115, pp. 172613.

[5] GICH, M., FRONTERA, C., ROIG, A., FONTCUBERTA, J., MOLIUS, E., BELLINDO, N., SIMON, C. FLETA, C. Magnetoelectric coupling in ε-$Fe_2O_3$ nanoparticles, *Nanotechnology*, 2006, vol. 17, no. 3, pp. 687-691.

[6] CARRARO, G., BARRECA, D, MACCATO, C., BONTEMPI, E., DEPRO, L.E., FERNANDEZ, C.J., CANESCHI, A. Supported ε and β iron oxide nanomaterials by chemical vapor deposition: structure, morphology and magnetic properties, *CrystEngComm*, 2013, vol.15, no. 6, pp. 1039-1042.

[7] MACHALA, L., TUCEK, J., ZBORIL, R. Polymorphous Transformations of Nanometric Iron(III) Oxide: A Review, *Chemistry of Materials*, 2011, vol.14, no.23, pp. 3255-3272.

[8] TUCEK,J., ZBORIL,R., NAMAI,A., OHKOSHI, S.I. ε-$Fe_2O_3$: An advanced nanomaterial exhibiting giant coercive field, millimeter-wave ferromagnetic resonance, and magnetoelectric coupling, *Chemistry of Materials*, 2010, vol. 22, no. 24, pp. 6483-6505.

[9] JIN, J., OHKOSHI, S., HASHIMOTO, K. Giant coercive field of nanometer-sized iron oxide, *Advanced Materials*, 2004, vol. 16, no 1, pp. 48-51.

[10] SAKURAI, S., JIN, J., HASHIMOTO, K., OHKOSHI, S. Reorientation phenomenon in a magnetic phase of ε-$Fe_2O_3$ nanocrystal, *Japanese Journal of Applied Physics*, 2005, vol. 74, no. 7, pp. 1946-1949.

[11] SAKURAI, S., KUROKI, H., TOKORO, K., HASHIMOTO, K., OHKOSHI, S. Synthesis, crystal structure, and magnetic properties of ε-$InxFe_2$-$xO_3$ nanorod-shaped magnets, *Advanced Functional Materials*, 2007, vol. 17, no. 14, pp. 2278-2282.

[12] SAKURAI, S., NAMAI, A., HASHIMOTO, K., OHKOSHI, S. First observation of phase transformation of all four $Fe_2O_3$ phases (γ→ε→β→α-phase), *Journal of the American Chemical Society*, 2009, vol. 131, no. 51, pp. 18299-18303.

[13] OHKOSHI, S., SAKURAI, S., JIN, J., HASHIMOTO, K. The addition e□ects of alkaline earth ions in the chemical synthesis of ε-$Fe_2O_3$ nanocrystals that exhibit a huge coercive field, *Journal of Applied Physics*, 2005, vol. 97, pp. 10K312.

[14] TRONC,E., CHANEAC,C., JOLIVET, J.P. Structural and Magnetic Characterization of ε-$Fe_2O_3$, *Journal of Solid State Chemistry*, 1998, vol. 139, no. 1, pp. 93-104.

[15] KURMOO,M., REHSPRINGER, J.L., HUTLOVA,A., DORLEANS,C., VILMINOT,S., ESTOURNES,C., NIZNANSKY,D. Formation of nanoparticles of ε-$Fe_2O_3$ from yttrium iron garnet in a silica matrix: An unusually hard magnet with a Morin-like transition below 150 K, *Chemistry of Materials*, 2005, vol. 17, no. 5, pp. 1106-1114.

[16] GICH,M., FRONTERA,C., ROIG,A., TABOADA,E.,MOLINS,E.,RECHENBERG,H.R., ARDISSON,J.D., MACEDO,W.A.A., RITTER,C., HARDY,V., SORT,J., SKUMRAYEV,V., NOGUES,J. High-and Low-Temperature Cristal and Magnetic Structures of ε-$Fe_2O_3$ and Their Correlation to Its Magnetic Properties, *Chemistry of Materials*, 2006, vol. 18, no. 16, pp. 3889-3897.

[17] CHANEAC,C., TRONC,E., JOLIVET, J.P. Thermal behavior of spinel iron oxide-silica composites, *Nanostructured Materials*, 1995, vol. 6, no. 5-8, pp. 715-718.

[18] BALAEV, D.A., DUBROVSKIY, A.A., SHAYHHUTDINOV, K.A., BAYUKOV, O.A., YAKUSHKIN, S.S., BUKHTIYAROVA ,G.A., MARTYANOV, O.N. Surface effects and magnetic ordering in few-nm-sized-$Fe_2O_3$ particles, *Journal of Applied Physics*, 2013, vol. 114, pp. 163911.

[19] NIKOLIC, V., SPASOJEVIC, V., PANJAN, M., KOPANJA, L., MRAKOVIC, A., TADIC, M. Re-formation of metastable ε-$Fe_2O_3$ in post-annealing of $Fe_2O_3/SiO_2$ nanostructure: Synthesis, computational particle shape analysis in micrographs and magnetic properties, *Ceramics International*, 2017, vol. 43, no. 10, pp. 7497-7507.

[20] SAKURAI, S., TOMITA, K., HASHIMOTO, K., YASHIRO, H., OHKOSHI S. Preparation of the nanowire form of ε-$Fe_2O_3$ single crystal and a study of the formation process. *Journal of Physical Chemistry C*, 2008, vol. 112, no 51, pp. 20212-20216.

[21] OHKOSHI, S., TOKORO, H. Hard Magnetic Ferrite: ε-$Fe_2O_3$, *Bulletin of the Chemical Society of Japan*, 2013, vol. 86, no. 8, pp. 897-907.

[22] KIM, D.K., ZHANG, Y., VOIT, W., RAO, K.V., MUHAMMED, M. Synthesis and characterization of surfactant-coated superparamagnetic monodispersed iron oxide nanoparticles, *Journal of Magnetism and Magnetic Materials*, 2001, vol. 225, no.1, pp. 30-36.

[23] POPOVICI, M., GICH, M., NIZNANSKY, D., ROIG, A., SAVII, C., CASAS, L., MOLINS, E., ENACHE, C., SORT, J., BRION, S., CHOUTEAU, G., NOGUES, D. Optimized Synthesis of the Elusive E-$Fe_2O_3$ Phase via Sol-Gel Chemistry, *Journal of Chemistry Materials,* 2004, vol. 25, no. 16, pp. 5544-5548.